Electrospray Ionization Mass Spectrometric Analyses of Phospholipids from Rat and Human Pancreatic Islets and Subcellular Membranes: Comparison to Other Tissues and Implications for Membrane Fusion in Insulin Exocytosis†

Sasanka Ramanadham, Fong-Fu Hsu, Alan Bohrer, William Nowatzke, Zhongmin Ma, and John Turk*

Mass Spectrometry Resource, Division of Diabetes, Endocrinology, and Metabolism, Department of Medicine, Washington University School of Medicine, 660 South Euclid Avenue, St. Louis, Missouri 63110

Received September 10, 1997; Revised Manuscript Received December 11, 1997

ABSTRACT: Glucose-induced insulin secretion from pancreatic islets involves hydrolysis of arachidonic acid from phospholipids as an intermediary event. Accumulation of nonesterified arachidonate in islet membranes may influence both ion fluxes that trigger insulin secretion and fusion of secretory granule and plasma membranes. Recent findings indicate that plasmenylethanolamine species may also participate in fusion of such membranes, but high-performance liquid chromatographic (HPLC) and gas chromatographic/mass spectrometric (GC/MS) analyses of islet secretory granule phospholipids suggested that they contain little plasmenylethanolamine. Here, electrospray ionization mass spectrometry (ESI/MS) of intact phospholipid molecules is used to demonstrate that the most prominent components of all major glycerophospholipid headgroup classes in islets are arachidonate-containing species. Such species contribute the majority of the ESI/MS negative ion current from rat and human islet glycerophosphoethanolamine (GPE), and the fraction of GPE negative ion current contributed by plasmenylethanolamine species in rat islets is higher than that for rat liver or heart and similar to that for brain. The most prominent *sn*-2 substituent of plasmenylethanolamine species in brain is docosahexaenoate and in islets is arachidonate. Arachidonate-containing plasmenylethanolamine species are also prominent components of GPE from islet secretory granules and plasma membranes. Fusion of islet secretory granule and plasma membranes is demonstrated to be catalyzed by cytosolic components from insulinoma cells and rat brain with chromatographic similarities to a rabbit brain factor that specifically catalyzes fusion of plasmenylethanolamine-containing membranes.

Type II diabetes mellitus, the most prevalent human endocrine disease, is characterized by impaired glucose-induced insulin secretion (*1*). Such secretion requires glucose transport into and metabolism within pancreatic islet β-cells (*2*, *3*), which yields signals, including changes in concentrations of ATP and ADP, that inactivate ATP-sensitive K^+ channels in β-cell plasma membranes (*4*, *5*). This induces membrane depolarization, opening of voltage-operated Ca^{2+} channels, and a rise in cytosolic [Ca^{2+}] that triggers insulin exocytosis (*6*−*8*). Glucose also induces phospholipid hydrolysis in β-cells and accumulation of nonesterified arachidonic acid (*9*−*12*), which facilitates Ca^{2+} entry and amplifies the rise in β-cell cytosolic [Ca^{2+}] and insulin secretion induced by depolarization (*10*, *13*, *14*). Inhibitors of phospholipase A_2 (PLA_2)[1] enzymes that hydrolyze arachidonate from islet phospholipids suppress both insulin secretion (*15*−*18*) and the rise in β-cell [Ca^{2+}] (*16*) induced by glucose, and both responses are restored by exogenous arachidonate (*16*−*18*).

These observations suggest that arachidonate and phospholipids that contain it may participate in β-cell function, and this is consistent with evidence that islet phospholipids are enriched in arachidonate. Gas chromatographic (GC)/mass spectrometric (MS) analyses of solvolysis products from islet phospholipids isolated by HPLC suggest that arachidonate comprises 30−36% of the total esterified fatty acyl mass of rat and human islet phospholipids (*19*, *20*). Because arachidonate is distributed predominantly in the *sn*-2 position of phospholipids that contain a distinct *sn*-1 substituent, this suggests that the majority of islet phospholipid molecules contain arachidonate. GC/MS analyses of phospholipid solvolysis products also suggest that islet glycerophosphoethanolamine (GPE) lipids contain a high fraction of plasmenylethanolamine species (*19*, *20*), which contain a vinyl ether linkage to a fatty aldehyde residue rather than

† This work was supported by U.S. Public Health Service Grants DK34388, RR00954, and S10-RR11260 and an American Diabetes Association Career Development Award (S.R.).

* Corresponding author: Box 8127, Washington University School of Medicine, 660 S. Euclid Ave., St. Louis, MO 63110. Telephone 314-362-8190; telefax 314-362-8188.

[1] Abbreviations: BSA, bovine serum albumin; CAD, collisionally activated dissociation; CL, cardiolipin; GC, gas chromatography; ESI, electrospray ionization; FAB, fast atom bombardment; GAPDH, glyceraldehyde-3-phosphate dehydrogenase; GPC, glycerophosphocholine; GPE, glycerophosphoethanolamine; GPI, glycerophosphoinositol; GPS, glycerophosphoserine; HBSS, Hanks' balanced salt solution; HEPES, 4-(2-hydroxyethyl)-1-piperazineethanesulfonic acid; HPLC, high-performance liquid chromatography; KRB, Krebs−Ringer bicarbonate buffer; MES, 2-(*N*-morpholino)ethanesulfonic acid; MOPS, 4-morpholinopropanesulfonic acid; NP, normal phase; MS, mass spectrometry; PBS, phosphate-buffered saline; PM, plasma membranes; R18, octadecylrhodamine; SG, secretory granules; SM, sphingomyelin.

S0006-2960(97)02250-2 CCC: $15.00
Published on Web 03/10/1998

an ester linkage to a fatty acid residue in the *sn*-1 position. Plasmenylethanolamine species are also abundant in neurons (*21*), and both neurons and β-cells are electrically active secretory cells with many biochemical similarities (*22*). Recent evidence indicates that the plasmenylethanolamine content of subcellular membranes may govern their ability to fuse (*23*, *24*), owing to the propensity of such molecules to adopt an inverted micellar phase (*25*) intermediate structure in membrane bilayer fusion (*26*). Fusion of plasma membranes with secretory granules in β-cells or with synaptic vesicles in neurons is the final step in exocytosis of insulin or neurotransmitters, respectively.

Previous analyses of islet phospholipid species have been indirect and involved two sequential HPLC steps, solvolysis, derivatization, and GC/MS (*19*, *20*). This can result in ambiguous assignments of species that are incompletely separated by HPLC and in underestimation of labile species lost during multiple processing steps, and it is desirable to characterize intact phospholipid molecules from islets directly. Fast atom bombardment (FAB) MS permits direct analysis of intact phospholipid molecules and structural characterization of all major headgroup classes (*27*), but the sensitivity of FAB/MS is limited by matrix-derived background ions. Islets comprise only 2% of pancreatic mass and must be isolated by a laborious procedure that yields only small quantities (*28*). This limits the utility of FAB/MS in analyzing islet phospholipids and precludes its application to islet subcellular membranes (*20*). Electrospray ionization (ESI) MS offers sensitivity superior to FAB/MS for phospholipid analysis and also permits direct characterization of phospholipid mixtures (*29*−*32*).

ESI/MS is used here to identify directly the major islet phospholipid species and to demonstrate that arachidonate-containing species are the most prominent components of the major glycerophospholipid headgroup classes. Islets exhibit a profile of phospholipid species distinct from some other tissues, and arachidonate-containing plasmenylethanolamine species are prominent components of glycerophosphoethanolamine (GPE) lipids of whole rat and human islets and of isolated islet secretory granules and plasma membranes. Fusion of islet secretory granule and plasma membranes is demonstrated to be catalyzed by cytosolic factors from insulinoma cells and rat brain that exhibit chromatographic behavior similar to that of a factor isolated from rabbit brain that specifically catalyzes fusion of plasmenylethanolamine-containing membranes (*23*, *24*).

EXPERIMENTAL PROCEDURES

Materials. Standard phospholipids were obtained from Avanti Polar Lipids (Birmingham, AL); organic solvents were from Burdick and Jackson (Muskegee, MI); buffer salts were from Sigma Chemical Co. (St. Louis, MO); HPLC columns were from Alltech (Deerfield, IL); male Sprague-Dawley rats were from Sasco (O'Fallon, MO); collagenase was from Boehringer Mannheim (Indianapolis, IN); tissue culture medium (CMRL-1066), penicillin, streptomycin, Hanks' balanced salt solution (HBSS), heat-inactivated fetal bovine serum, and L-glutamine were from Gibco (Grand Island, NY); pentex bovine serum albumin (fatty acid free, fraction V) was from Miles Laboratories (Elkhart, IN); rodent chow 5001 was from Ralston Purina (St. Louis, MO); D-glucose was from the National Bureau of Standards (Washington, DC); and HIT-T15 insulinoma cells were from ATCC (Bethesda, MD). Media included KRB (Krebs−Ringer bicarbonate buffer: 25 mM HEPES, pH 7.4, 115 mM NaCl, 24 mM $NaHCO_3$, 5 mM KCl, 2.5 mM $CaCl_2$, and 1 mM $MgCl_2$), cCMRL-1066 [CMRL-1066 supplemented with 10% heat-inactivated fetal bovine serum, 1% L-glutamine, and 1% (w/v) each penicillin and streptomycin]; and HBSS (Hanks' balanced salt solution supplemented with 0.5% penicillin−streptomycin).

Isolation of Pancreatic Islets. Islets were isolated from male Sprague-Dawley rats (200 g body weight) after pancreatic excision, collagenase digestion, and centrifugation through a discontinuous Ficoll gradient as described elsewhere (*28*). Isolated islets were resuspended in cCMRL-1066 medium, transferred into Falcon Petri dishes containing 2.5 mL of cCMRL-1066, and placed under an atmosphere of 95% air/5% CO_2 at 37 °C. Human pancreatic islets were prepared in the Core Laboratory of the Washington University Diabetes Research and Training Center (*33*) and cultured at 37 °C under an atmosphere of 5% CO_2/95% O_2 in CMRL-1066 containing 10% fetal bovine serum, penicillin (100 units/mL), glutamine (2 mM), and HEPES (25 mM) at pH 7.4.

Preparation of Insulin Secretory Granules by Percoll Density Gradient Analysis. Insulin secretory granules were prepared as described (*20*, *34*) from islets homogenized in a Potter-Elvehjem tissue grinder in SG buffer [260 mM sucrose and 10 mM MOPS (4-morpholinopropanesulfonic acid), pH 6.5]. The homogenate (H) was diluted with SG buffer and centrifuged (900*g*, 5 min). The supernatant (S_1) was centrifuged (13000*g*, 10 min) and the resultant supernatant (S_2) was layered atop Percoll density gradients consisting of a 50 μL layer of 100% Percoll and a 250 μL layer of 35% Percoll. After centrifugation (13000*g*, 10 min), the lower 150 μL of the gradient, which contained insulin secretory granules (SG) (*20*, *34*), was removed. The Percoll content of the SG fraction was reduced by dilution in SG buffer and centrifugation (13000*g*, 10 min). Aliquots of all fractions were removed for measurement of protein, acid-extractable insulin, and 5′-nucleotidase activity. Phospholipids in the SG fraction was analyzed as described below.

Preparation of Islet Cell Plasma Membranes and Endoplasmic Reticulum by Sucrose Density Gradient Analysis. Islet plasma membranes and endoplasmic reticulum were prepared as described (*20*, *28*) from islets homogenized as above in fractionation buffer [50 mM MES [2-(*N*-morpholino)ethanesulfonic acid] and 250 mM sucrose, pH 7.2]. The homogenate was centrifuged (600*g*, 5 min), and the supernatant (S_1) was transferred to a separate tube. The pellet (P_1) was suspended in fractionation buffer and centrifuged (600*g*, 5 min). This supernatant was combined with S_1 and centrifuged (20000*g*, 20 min). The resulting supernatant (S_2) was diluted with fractionation buffer and the pellet (P_2) was suspended in 10 mM MES with 1 mM EGTA (pH 6.0). S_2 was centrifuged (150000*g*, 90 min) to yield a supernatant (S_4) and pellet (P_4). P_4 is enriched in endoplasmic reticulum (ER) (*28*) and was resuspended in fractionation buffer and rehomogenized. P_2 was homogenized and layered atop a discontinuous sucrose gradient (with layer densities of 1.14, 1.16, 1.18, and 1.20) and centrifuged (150000*g*, 90 min). The bands collecting at the top two interfaces contain plasma

membranes (PM) (*28*) and were collected, suspended in buffer (10 mM MES and 1.0 mM EGTA, pH 6.0), centrifuged (150000*g*, 60 min), and suspended in buffer (10 mM MES, pH 6.0). Aliquots of all fractions were removed for determination of protein, insulin, and 5′-nucleotidase activity. Phospholipids in the PM and ER fractions were analyzed as described below.

Characterization of Islet Subcellular Membrane Preparations. Membrane-enclosed insulin was extracted with 40 μL of 1.5% sulfuric acid in 75% ethanol (overnight, 4 °C), as described (*28*) and insulin was measured by radioimmunoassay. Activity of the plasma membrane enzyme 5′-nucleotidase was determined by a modification (*35*) of a described method (*36*). Protein was measured with Coomassie protein assay reagent (Pierce, Rockford, IL) against a BSA standard.

Extraction of Islet Phospholipids. Phospholipids from rat and human islets and subcellular membranes were extracted with chloroform/methanol under neutral conditions (*37*). Islets or subcellular membranes in 0.8 mL of buffer were placed in silanized 10 mL glass tubes. Methanol (2 mL) and chloroform (1 mL) were added and the tubes were mixed after each addition and then sonicated on ice with a Branson sonifier. Water (1 mL) and chloroform (1 mL) were added and the tubes were mixed after each addition and then centrifuged (800*g*, 5 min). The chloroform (lower) phase was removed, concentrated to dryness, and reconstituted in methanol/chloroform (9/1).

Preparation of Other Rat Tissues and Extraction of Their Phospholipids. Male Sprague-Dawley rats (200 g body weight) were anesthetized with intraperitoneal sodium pentobarbital, and liver, heart, and brain were removed. Tissue samples were minced and rinsed twice in ice-cold phosphate-buffered saline (PBS). Minced tissue (1 g wet weight) was placed in a solution (2 mL) of chloroform/methanol (1/1 v/v) and homogenized (Tissue Tearor, setting 7, 60 s, Biospec Products, Bartlesville, OK). Homogenates were sonicated on ice (20% power, 5 s bursts for 60 s, Vibra Cell probe sonicator, Sonics and Materials, Danbury, CT). Samples were centrifuged (2800*g*, 5 min) to remove tissue debris and supernatants were transferred to silanized 10 mL glass tubes and extracted by adding methanol (1 mL), chloroform (1 mL), and water (1.8 mL). Samples were vortex-mixed and centrifuged (900*g*, 5 min) and the chloroform phase was removed, concentrated, and dissolved in methanol/chloroform (9/1).

Normal-Phase HPLC Isolation of Glycerophosphoethanolamine and Glycerophosphocholine Lipids from Phospholipid Extracts. GPE and GPC lipids were isolated from crude phospholipid extracts by normal phase HPLC (*38*) on a silicic acid HPLC column (LiChrosphere Si-100, 10 μm particle size, 250 × 4.6 mm, Alltech, Deerfield, IL) in a solvent system consisting of a gradient between solvent mixtures A and B, the compositions of which were hexane/2-propanol/water [100/100/3 100/100/7 (v/v/v), respectively]. The initial solvent composition (100% A/0% B) was maintained for 6 min (flow rate 2 mL/min) and followed by a linear gradient over 24 min to the final composition (50% A/50% B). Retention times for phospholipid standards were as follows: GPE, 8 min; GPI, 25 min; GPS, 30 min; and GPC, 55 min.

Determination of Acid Lability of Phospholipids. Acid lability of phospholipids was determined essentially as previously described (*19*, *20*, *39*, *40*). Phospholipid samples were divided into aliquots and concentrated to dryness. One aliquot was treated with acid [1 N HCl in methanol/chloroform (1/1 v/v), 1 mL, 45 min, room temperature], and the other was sham-treated [chloroform/methanol (1/1 v/v), 1 mL]. Samples were neutralized (1 M Na_2CO_3, 0.5 mL), extracted (chloroform, 1 mL), concentrated, reconstituted [methanol/chloroform (1/9 v/v), 0.1 mL], and analyzed by ESI/MS. Diacyl and alkylacyl phospholipids are acid-stable and appear in ESI/MS spectra of both acid- and sham-treated samples. Plasmalogens are acid-labile and do not appear in ESI/MS spectra of acid-treated samples (*39*).

Mass Spectrometry. ESI/MS analyses were performed on a Finnigan (San Jose, CA) TSQ-7000 triple-stage quadrupole tandem mass spectrometer with an ESI source controlled by Finnigan ICIS software operated on a DEC α workstation. Phospholipids were dissolved in methanol/chloroform (9/1 v/v) at final concentrations of about 1−5 pmol/μL. To facilitate formation of anionic species for negative ion analyses and to form lithiated adducts of GPC species for positive ion analyses, LiOH (2−5 nmol/μL) was added to this solution. Under these conditions, GPC species yield much greater signals in positive than in negative ion mode, and the converse is true for GPE species. For example, ESI/MS analysis of an equimolar mixture (5 pmol/μL) of standard dimyristoyl-GPC [(14:0/14:0)-GPC] and of standard (1-stearoyl-2-arachidonoyl)-GPE [(18:0/20:4)-GPE] in positive ion mode in the presence of LiOH yielded a signal of 3.01 × 10^6 counts for the $(MLi)^+$ ion (*m*/*z* 684) of (14:0/14:0)-GPC and no detectable signal (<0.06 × 10^6 counts) for the $(MLi)^+$ or $(MH)^+$ ions (18:0/20:4)-GPE at *m*/*z* 768 or 774, respectively. In contrast, analysis of the same sample in negative ion mode yielded a signal of 5.43 × 10^5 counts for the $(M - H)^-$ ion (*m*/*z* 766) of (18:0/20:4)-GPE and a signal of only 0.11 × 10^5 counts for the $(M - 15)^-$ ion (*m*/*z* 662) of (14:0/14:0)-GPC.

Samples were infused (1 μL/min) into the ESI source with a Harvard syringe pump. The electrospray needle and the skimmer were operated at ground potential. For acquisition of positive or negative ions, respectively, the electrospray chamber and the entrance of the glass capillary were operated at a positive or negative potential of 4.4 kV; a positive or negative 90 V potential was applied to the exit of the glass capillary; and a positive or negative 175 V potential was placed on the tube lens. The temperature of the heated capillary was 250 °C. For collisionally activated dissociation (CAD) and tandem mass spectrometry, precursor ions were selected in the first quadrupole and passed into the collision chamber containing argon (2.2−2.5 mTorr) at collision energies of 32−36 eV. Product ions were analyzed by *m*/*z* value in the final quadrupole. Product ion spectra were acquired using a signal-averaging protocol in profile mode at a rate of 1 scan/3 s. In addition to obtaining full-scan tandem mass spectra of product ions, tandem MS scanning experiments were performed to identify parent ions that either yielded product ions of a defined *m*/*z* value or underwent neutral losses of a defined value.

Preparation of Cytosol from HIT-T15 Insulinoma Cells and Rat Brain. HIT-T15 cells were detached from T-175 flasks with 0.05% trypsin/0.02% EDTA, washed with PBS,

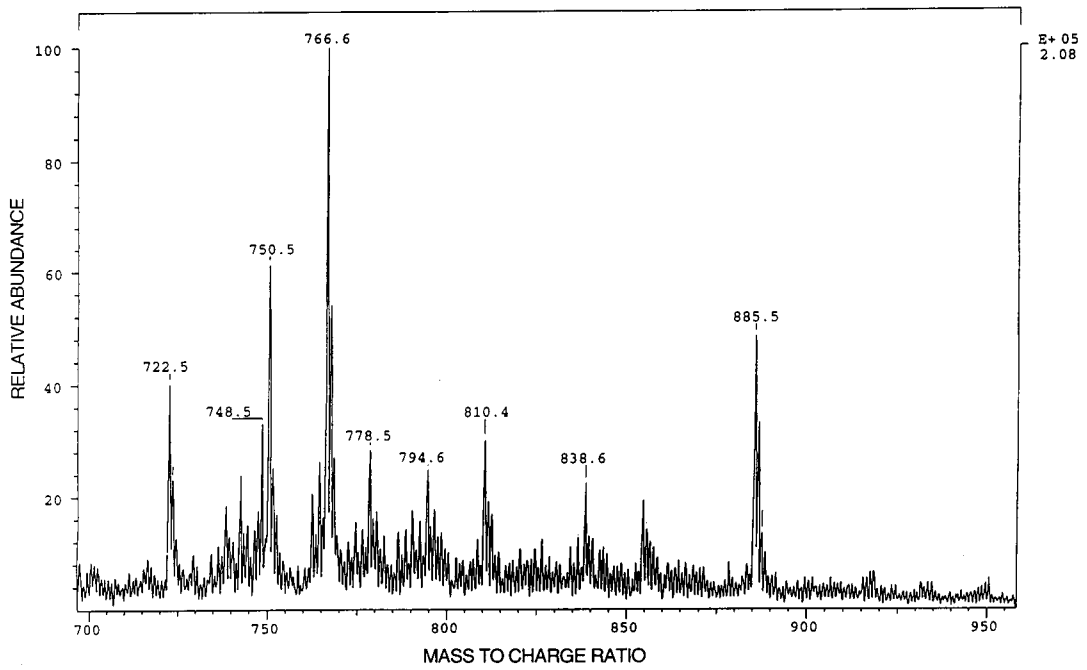

FIGURE 1: Electrospray ionization negative ion mass spectrometric analysis of phospholipids from isolated rat pancreatic islets. The spectrum is the ESI/MS total negative ion current of phospholipids extracted from isolated rat pancreatic islets.

collected by centrifugation, and disrupted by sonication (Vibra Cell, high-intensity ultrasonic processor, 15 × 1 s pulses, amplitude 12%) in buffer A (0.25 M sucrose, 50 mM Tris-HCl, 10 mM EGTA, 2 mM EDTA, and 1 mM DTT, pH 7.4). Rat brain tissue was homogenized (3 × 15 s bursts, setting 6, Polytron apparatus) in buffer A and disrupted by sonication (45 × 15 s pulses). Homogenates were centrifuged (170000*g*, 60 min) to yield a cytosolic supernatant. Crude cytosol was dialyzed overnight, with a buffer change after 6 h, against buffer B (50 mM Tris, 0.1 mM EGTA, 0.1 mM EDTA, and 1 mM DTT, pH 7.0).

Anion-Exchange Chromatographic Analysis of Cytosol from HIT-T15 Insulinoma Cells and Rat Brain. Chromatographic analyses of cytosol were performed as previously described (24) by applying dialyzed cytosol to a DE-52 (Whatman International Ltd., Fairfield, NJ) anion-exchange column (2.6 cm × 20 cm) previously equilibrated with buffer B. Elution by gravity was performed with buffer B, and aliquots of eluant fractions were assayed for ability to catalyze fusion of isolated insulin secretory granules and islet plasma membranes, as described below.

Monitoring of Fusion of Isolated Insulin Secretory Granule Membranes with Islet Plasma Membranes. Membrane fusion was monitored by a fluorescence-dequenching assay in which the lipid-soluble fluorophore octadecylrhodamine B (R18) is incorporated into membranes (*41*). The fluorescent signal from R18 is limited by self-quenching, which is proportional to its surface density in membranes. Fusion of R18-labeled membranes with unlabeled membranes decreases R18 surface density and yields proportional increases in fluorescence intensity (*41*). Secretory granule suspensions were diluted in 9 volumes of reaction buffer (111 mM KCl, 3 mM $MgCl_2$, 22 mM sucrose, 11 mM Tris-HCl, pH 7.4, and 1 mM EGTA) and incubated (6 min, 37 °C, in the dark) with R18 (60 μM). R18-labeled secretory granules were collected by centrifugation (1450*g*, 10 min) and resuspended in reaction buffer. An aliquot of R18-labeled secretory granules (3 μg of protein) and unlabeled islet plasma membranes (1 μg of protein) were added to a cuvette containing reaction buffer (total volume 1.6 mL). Fluorescence was monitored at 37 °C with constant stirring in an SLM Aminco (SPF-500C) spectrofluorometer with excitation and emission wavelengths of 560 nm (band-pass 2 nm) and 590 nm (band-pass 10 nm), respectively. After a steady baseline fluorescence signal was achieved, aliquots of eluant from DE-52 anion exchange chromatographic analysis of dialyzed cytosol from HIT-T15 insulinoma cells or from rat brain was added. Fluorescence signal was then monitored for 10 min.

RESULTS

Figure 1 illustrates the total negative ion current profile from ESI/MS analysis of phospholipids extracted from freshly isolated rat pancreatic islets. Each major ion in this spectrum was subjected to collisionally activated dissociation (CAD) and tandem mass spectrometry, and Figure 2 contains structural diagrams of some of the lipids identified in islet extracts. Most of the ions in Figure 1 have even nominal *m*/*z* values, indicating that they contain an odd number of nitrogen atoms, consistent with glycerolipids that contain ethanolamine, serine, or choline headgroups.

An exception is the ion at *m*/*z* 885, which has an odd nominal mass value. The CAD tandem mass spectrum of this ion is illustrated in Figure 3A, and it represents 1-stearoyl-2-arachidonoylglycerophosphoinositol [(18:0/20:4)-GPI], the structure of which is illustrated in Figure 2A. The spectrum (Figure 3A) contains stearate (*m*/*z* 283) and arachidonate (*m*/*z* 303) anions, an ion (*m*/*z* 241) representing a dehydration product of inositol phosphate, ions reflecting neutral losses of arachidonate as a free fatty acid (*m*/*z* 581) or as a substituted ketene (*m*/*z* 599), and an ion (*m*/*z* 419) reflecting neutral losses of inositol and of arachidonic acid as a ketene. Figure 1 suggests that (18:0/20:4)-GPI (*m*/*z* 885) is the predominant GPI species in islets, as no ions of

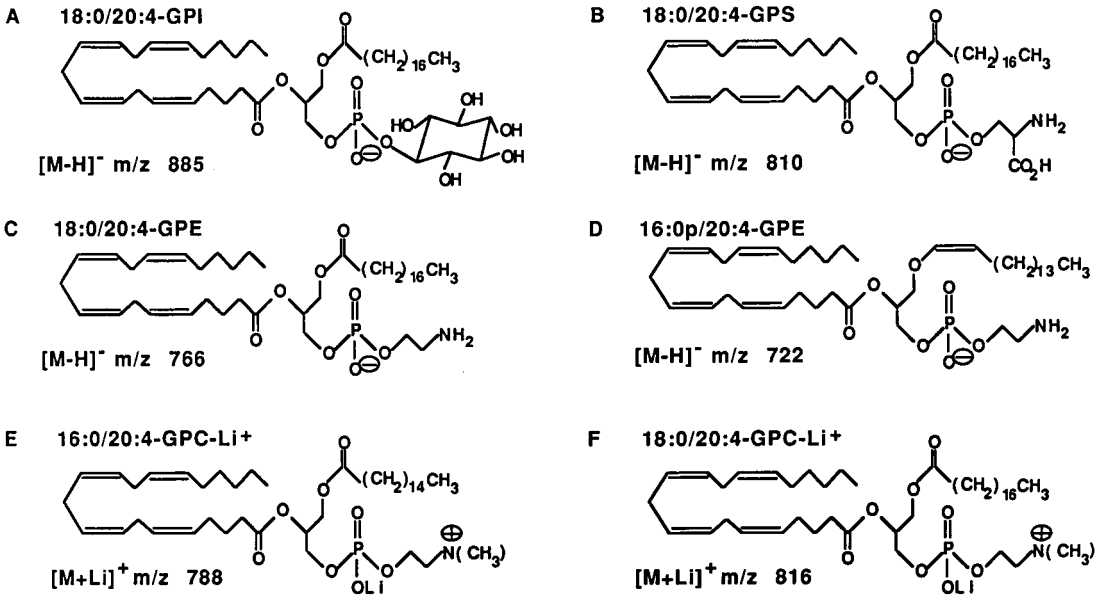

FIGURE 2: Structural diagrams of some of the more abundant phospholipid molecular species identified in pancreatic islets by electrospray ionization tandem mass spectrometry.

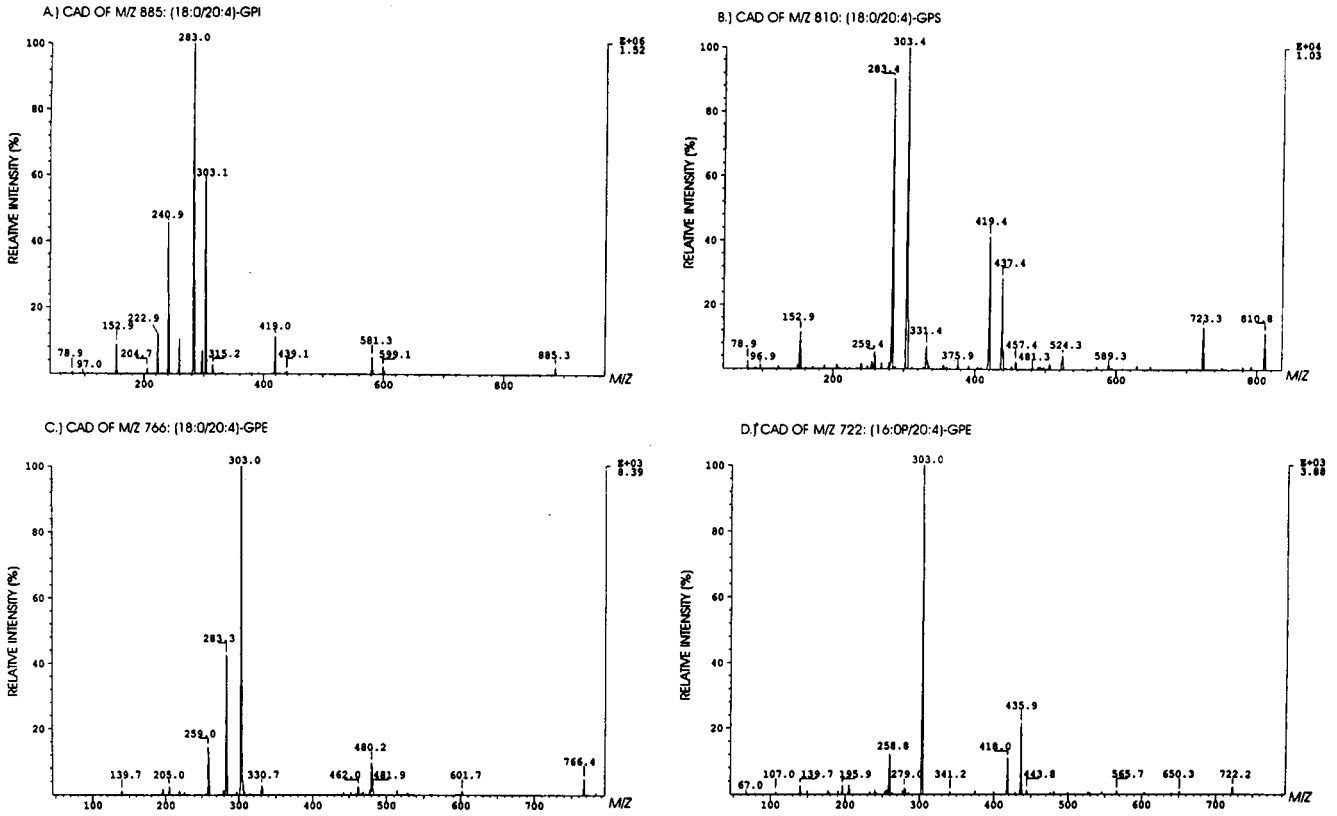

FIGURE 3: Tandem negative ion mass spectra obtained from some of the more abundant phospholipid molecular species in isolated pancreatic islets. Each spectrum was obtained upon CAD of one of the parent ions from the islet phospholipid mixture in Figure 1: Panel A is the tandem spectrum of the ion at *m/z* 885 and represents 1-stearoyl-2-arachidonoylglycerophosphoinositol. Panel B is the tandem spectrum of the ion at *m/z* 810 and represents 1-stearoyl-2-arachidonoylglycerophosphoserine. Panel C is the tandem spectrum of the ion at *m/z* 766 and represents 1-stearoyl-2-arachidonoylglycerophosphoethanolamine. Panel D is the tandem spectrum of the ion at *m/z* 722 and represents the plasmenylethanolamine species with residues of palmitic aldehyde and of arachidonic acid in the *sn*-1 and *sn*-2 positions, respectively.

comparable abundance with odd nominal *m/z* values occur in the range expected for GPI species with other common fatty acid substituents. The predominance of (18:0/20:4)-GPI among islet GPI species was supported by tandem MS scanning experiments to identify precursors of the product ion *m/z* 241 in islet lipid extracts. This ion is common to the tandem spectra of GPI species (*27*), and *m/z* 885 was the only parent ion of substantial abundance observed in such scans with islet phospholipids.

The ions at *m/z* 810 and 838 in Figure 1 correspond to glycerophosphoserine (GPS) species. The tandem mass spectrum obtained from CAD of the ion at *m/z* 810 is illustrated in Figure 3B, and it represents (18:0/20:4)-GPS, the structure of which is illustrated in Figure 2B. The

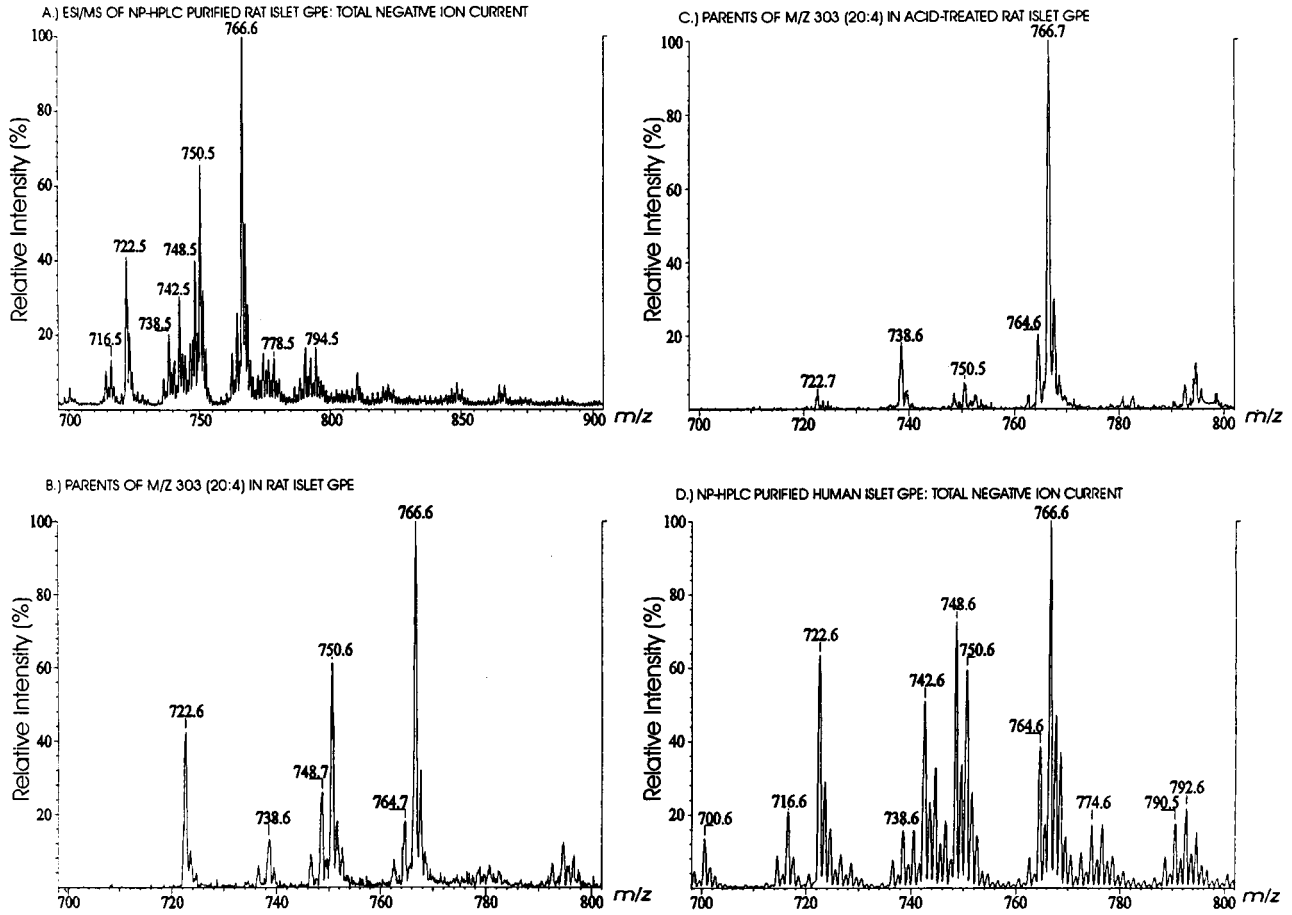

FIGURE 4: Electrospray ionization negative ion mass spectrometric analysis of pancreatic islet glycerophosphoethanolamine lipids. Phospholipids extracted from rat (panels A−C) or human (panel D) pancreatic islets were analyzed by NP-HPLC to isolate GPE lipids, which were then analyzed by negative ion ESI/MS. Panel A is the total negative ion current for rat islet GPE. Panels B and C represent tandem MS scanning experiments in which parent ions from non-acid-treated (panel B) or acid-treated (panel C) rat islet GPE lipids were identified that yield the arachidonate anion (*m*/*z* 303) upon CAD. Panel D is the total negative ion current for human islet GPE.

spectrum (Figure 3B) contains stearate (*m*/*z* 283) and arachidonate (*m*/*z* 303) anions, a phosphatidate anion (*m*/*z* 723, loss of 87) reflecting loss of a dehydration product of serine from the $(M - H)^-$ ion, and ions reflecting neutral losses of arachidonate as a free fatty acid (*m*/*z* 419) or as a substituted ketene (*m*/*z* 437) from the phosphatidate ion. Analogous product ions in the tandem mass spectrum of the parent ion at *m*/*z* 838 in Figure 1 indicated that this ion represents (18:0/22:4)-GPS. Figure 1 suggests that (18:0/20:4)-GPS is the most abundant and (18:0/22:4)-GPS is the next most abundant GPS species in islet lipid extracts. This was supported by tandem MS scanning experiments to identify parent ions that undergo neutral loss of 87. This loss is common to GPS species (*27*), and *m*/*z* 810 and 838 were the only parent ions of substantial abundance observed in such scans with islet extracts.

The major contributors to the ions at *m*/*z* 722, 738, 748, 750, 764, 766, 778, and 794 in Figure 1 are glycerophosphoethanolamine (GPE) species, and two series of compounds are represented among them. The first consists of diacyl-GPE species and the second of ether-linked GPE species. CAD of the ion at *m*/*z* 766 in Figure 1 yielded the tandem mass spectrum illustrated in Figure 3C, and it represents the diacyl species (18:0/20:4)-GPE, the structure of which is illustrated in Figure 2C. This spectrum contains stearate (*m*/*z* 283) and arachidonate (*m*/*z* 303) anions and an ion (*m*/*z* 480) reflecting loss of arachidonate as a ketene. Similar tandem mass spectra of the peaks at *m*/*z* 738, 764, and 794 in Figure 1 identified the parents as the diacyl species (16:0/20:4)-GPE, (18:1/20:4)-GPE, and (18:0/22:4)-GPE, respectively. CAD of the ion at *m*/*z* 722 yielded the tandem mass spectrum illustrated in Figure 3D, and it is consistent with the plasmalogen species (16:0p/20:4)-GPE (Figure 2D) in which the *sn*-1 substituent is a residue of palmitic aldehyde. Prominent ions in its tandem spectrum (Figure 3D) include the arachidonate anion (*m*/*z* 303) and ions reflecting loss of arachidonate as a free fatty acid (*m*/*z* 418) or as a ketene (*m*/*z* 436). Both of the GPE tandem spectra in Figure 3 exhibit ions of low abundance at *m*/*z* 196 and 140, consistent with a dehydration product of the glycerophosphoethanolamine moiety (*30*) and phosphoethanolamine anion (*27*), respectively. Similar tandem mass spectra of the peaks at *m*/*z* 748, 750, and 778 in Figure 1 were consistent with the plasmalogen species (18:1p/20:4)-GPE, (18:0p/20:4)-GPE, and (18:0p/22:4)-GPE, respectively. Although these tandem mass spectra would also be consistent with alkyl-ether GPE species with residues of unsaturated fatty alcohols as *sn*-1 substituents, assignment of the indicated species as plasmalogens was achieved by acid-lability studies (*27*, *39*), as described below.

Although, as summarized in Experimental Procedures, glycerophosphocholine (GPC) species yield much stronger signals on positive ion than on negative ion ESI/MS analyses, GPC species do yield some $(M - 15)^-$ ions on negative ion

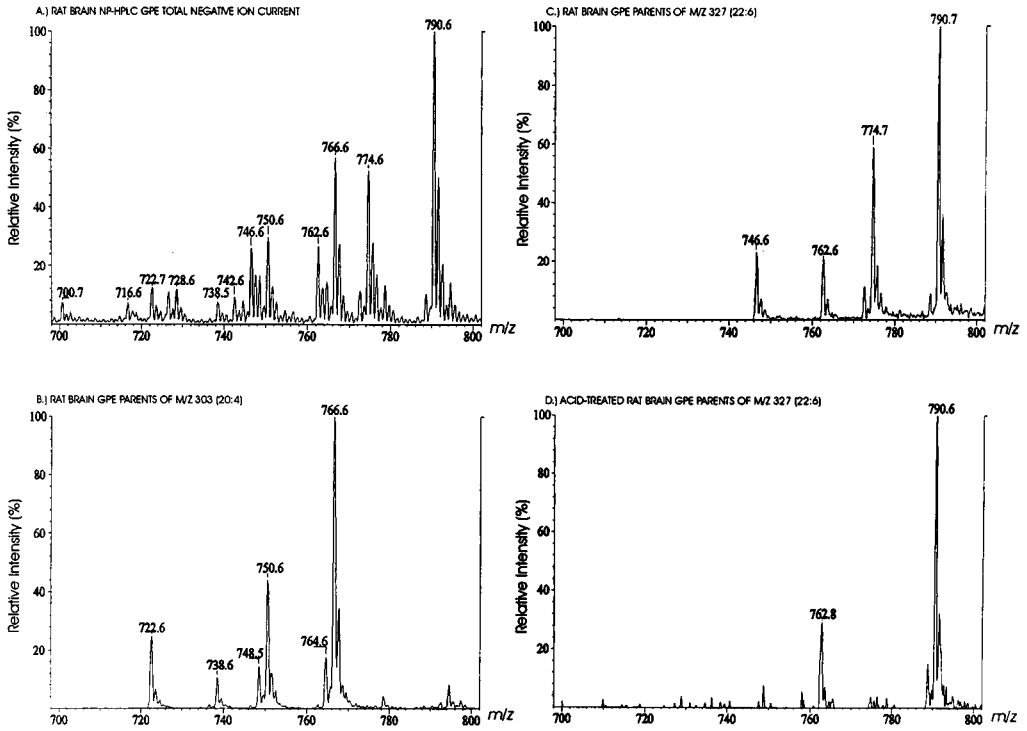

FIGURE 5: Electrospray ionization negative ion mass spectrometric analysis of rat brain glycerophosphoethanolamine lipids. Rat brain phospholipid extracts were analyzed by NP-HPLC to isolate GPE lipids, which were then analyzed by negative ion ESI/MS. Panel A is the total negative ion current profile. Panels B−D represent tandem MS scanning experiments in which parent ions from non-acid-treated (panels B and C) or acid-treated (panel D) brain GPE were identified that yield arachidonate anion (*m*/*z* 303) (panel B) or docosahexaenoate anion (*m*/*z* 327) (panels C and D) upon CAD.

FAB/MS (27) and ESI/MS. In some cases, such ions can be confused with $(M - H)^-$ ions from GPE species. For example, the $(M - 15)^-$ ion from (16:0/20:4)-GPC and the $(M-H)^-$ ion from (18:0/20:4)-GPE both have an *m*/*z* value of 766. Islet GPE species were therefore isolated by normal-phase (NP) HPLC, which separates phospholipids into headgroup classes (*38*), and then analyzed by negative ion ESI/MS. The resultant profile (Figure 4A) includes all major ions thought to represent GPE species from tandem MS analyses with the crude islet extract (Figures 1 and 3), and the relative abundances of the major ions in the *m*/*z* range 700−800 in Figures 1 and 4A are similar. This suggests that the major contributors to peaks in Figure 1 thought to represent GPE species are $(M - H)^-$ ions of GPE species and not $(M - 15)^-$ ions of GPC species because islets fail to express GPC species that would produce $(M - 15)^-$ ions corresponding to some of the more abundant ions attributed to GPE species in the profiles in Figures 1 and 4A, including those at *m*/*z* 750 and 722, as discussed further below.

The tandem MS scanning experiment with NP-HPLC-purified islet GPE illustrated in Figure 4B illustrates that each of the most abundant GPE species in islets contains arachidonate. This figure represents a scan in which precursor ions were identified that yield the arachidonate anion (*m*/*z* 303) as a product upon CAD. The relative intensities of the major peaks in Figure 4B are similar to those in the total negative ion current profile in Figure 4A, reflecting the predominance of arachidonate-containing species among islet GPE molecules. The vinyl ether linkage of plasmalogens is sensitive to acid (*27*, *39*), and acid-lability studies indicated that the prominent islet GPE species represented by the ions at *m*/*z* 722, 748, and 750 are plasmalogens (Figure 4C). Exposure of NP-HPLC-purified islet GPE to acid before negative ion ESI/MS analyses reduced abundances of the ions at *m*/*z* 722, 748, and 750 by about 10-fold relative to the ion at *m*/*z* 766 (Figure 4C), which represents an acid-stable diacyl-GPE species. Findings in Figure 4 thus indicate that the predominant components of rat islet GPE are arachidonate-containing species and include plasmalogens as major components.

This is also true for human islets, as illustrated in Figure 4D, which represents the ESI/MS total negative ion current from NP-HPLC-purified human islet GPE. Ions representing arachidonate-containing plasmenylethanolamine species (*m*/*z* 722, 748, and 750) and arachidonate-containing diacyl-GPE species (*m*/*z* 738, 764, and 766) are prominent in this spectrum. The identities of the species represented by these ions were confirmed by tandem mass spectra and acid-lability studies similar to those described above (not shown). To compare profiles of GPE species expressed in islets to those of other rat tissues, NP-HPLC-purified GPE lipids from brain (Figure 5), liver (Figure 6A,B), and heart (Figure 6C,D) were analyzed by negative ion ESI/MS and Table 1 summarizes the relative intensities of ions and the identities of the GPE species that they represent for rat and human islets and other rat tissues.

Figure 5A illustrates the negative ion ESI/MS profile of NP-HPLC-purified rat brain GPE, and ions in this spectrum represent series of diacyl-GPE and of plasmenylethanolamine species. In contrast to islet GPE species, in which arachidonate is the predominant *sn*-2 substituent, the more prominent *sn*-2 substituent in brain GPE is docosahexenoate, as illustrated in Figure 5B,C. Figure 5B represents a tandem MS scanning experiment in which parent ions in the brain GPE mixture were identified that yield the arachidonate anion (*m*/*z* 303) as a product upon CAD. This profile is similar to

Table 1: Negative Ion Electrospray Inization Mass Spectrometric Analysis of Glycerophosphoethanolamine Species Isolated by Normal-Phase HPLC Analysis of Phospholipid Extracts from Rat and Human Pancreatic Islets and from Rat Brain, Liver, and Heart[a]

		relative intensity				
m/*z*	assignment	rat islets	rat brain	rat liver	rat heart	human islets
700	16:0p/18:1-GPE	NA	06	NA	NA	13
714	16:0/18:2-GPE	04	NA	42	11	08
716	16:0/18:1-GPE	04	07	09	05	20
722	16:0p/20:4-GPE	38	12	02	29	64
726	18:0p/18:2-GPE	NA	09	NA	NA	06
728	18:0p/18:1-GPE	NA	15	NA	NA	02
738	16:0/20:4-GPE	15	07	44	24	16
742	18:0/18:2-GPE	25	09	44	38	52
746	16:0p/22:6-GPE	NA	28	NA	24	15
748	18:1p/20:4-GPE	38	15	NA	38	73
750	18:0p/20:4-GPE	63	29	04	30	61
762	16:0/22:6-GPE	08	26	69	36	06
764	18:1/20:4-GPE	21	15	56	24	39
766	18:0/20:4-GPE	100	59	100	100	100
774	18:0p/22:6-GPE	08	53	NA	18	15
778	18:0p/22:4-GPE	07	12	NA	08	08
790	18:0/22:6-GPE	10	100	32	84	16
792	18:0/22:5-GPE	06	19	14	28	20
794	18:0/22:4-GPE	10	12	NA	16	16
	Fraction of Tabulated GPE Ion Current Represented by					
	20:4-containing species	0.77	0.32	0.49	0.47	0.64
	plasmalogen species	0.43	0.41	0.01	0.28	0.47
	plasmalogens with 20:4	0.39	0.13	0.01	0.13	0.36

[a] Bligh-Dyer lipid extracts from each tissue analyzed by NP-HPLC and GPE lipids were collected separately, concentrated, and analyzed by ESI/MS in negative ion mode. The relative intensity of each $(M - H)^-$ ion was determined from the total negative ion current profile. The identity of each molecular species was determined by CAD of $(M - H)^-$ ions and tandem mass spectrometry. Assignments were confirmed by linked-scanning tandem MS experiments to identify parents of specific fatty acid carboxylate anions. Plasmalogen species are identified by the letter p following the designation of the carbon chain length and number of carbon−carbon double bonds of the fatty aldehyde residue in the *sn*-1 position, e.g., 18:0p/20:4-GPE. All species not bearing this designation are diacyl species, and the carbon chain length and number of carbon−carbon bonds of the fatty acid residues in the *sn*-1 and *sn*-2 positions are specified. Minor isobaric contributors to some of the ions in the total ion current have not been included in the table.

that in Figure 4B for islet arachidonate-containing GPE species, except that the ions representing arachidonate-containing plasmenylethanolamine species (at *m*/*z* 722, 748, and 750) are somewhat less abundant relative to those representing arachidonate-containing diacyl-GPE species (at *m*/*z* 738, 764, and 766) for rat brain (Figure 5B) than for rat islet GPE (Figure 4B). Tandem mass spectra of these ions and acid-lability studies (not shown) confirmed their assignments (Table 1).

Figure 5C represents a similar tandem MS scanning experiment in which parent ions in the brain GPE mixture were identified that yield docosahexenoate anion (*m*/*z* 327) as a product upon CAD. This profile is similar in character to that in Figure 5B, and the four most abundant ions represent the two diacyl-GPE species (16:0/22:6)-GPE (*m*/*z* 762) and (18:0/22:6)-GPE (*m*/*z* 790) and the two plasmenylethanolamine species (16:0p/22:6)-GPE (*m*/*z* 746) and (18:0p/22:6)-GPE (*m*/*z* 774). Assignments of these plasmalogen species were confirmed by acid-lability studies (Figure 6D), which resulted in virtual disappearance of the ions at *m*/*z* 746 and 774, although the relative abundance of ions representing the diacyl-GPE species at *m*/*z* 762 and *m*/*z* 790 was little affected. These findings indicate that rat brain GPE contains two series of plasmenylethanolamine species with either arachidonate or docosahexaenoate as *sn*-2 substituent, and the total negative ion current profile in Figure 5A indicates that the latter series is more prominent than the former.

Figure 6A illustrates the negative ion ESI/MS profile obtained from NP-HPLC-isolated rat liver GPE. The major contributors to this spectrum are diacyl-GPE species (Table 1), and no prominent ions representing plasmenylethanolamine species are observed, confirming the reported paucity of plasmalogens in liver (*42*). The low abundance of arachidonate-containing plasmenylethanolamine species in liver is illustrated in Figure 6B, which represents a tandem MS experiment in which parent ions were identified that yield the arachidonate anion (*m*/*z* 303) as a product upon CAD. Comparison of Figures 6B and 4B indicates that, in contrast to islets, liver contains little (16:0p/20:4)-GPE (*m*/*z* 722), (18:1p/20:4)-GPE (*m*/*z* 748), or (18:0p/20:4)-GPE (*m*/*z* 750), relative to the predominant diacyl species (18:0/20:4)-GPE (*m*/*z* 766).

Figure 6C represents the negative ion ESI/MS profile for NP-HPLC-isolated heart GPE, and Figure 6D represents a tandem MS scanning experiment in which parent ions were identified that yielded the docosahexaenoate anion (*m*/*z* 327) as a product upon CAD. The two most abundant ions in Figure 6D represent the diacyl species 16:0/22:6-GPE (*m*/*z* 762) and 18:0/22:6-GPE (*m*/*z* 790). Two plasmenylethanolamine species, as confirmed by tandem mass spectra and acid-lability studies (not shown), are also represented in Figure 6D by the ions at *m*/*z* 746 [(16:0p/22:6)-GPE] and *m*/*z* 774 [(18:0p/22:6)-GPE], although their abundance relative to the diacyl-GPE species is lower than that for rat brain (Figure 5C). Similar tandem MS scanning experiments to identify parents of the arachidonate anion at *m*/*z* 303 also yielded a profile of ions that included both diacyl-GPE and plasmenylethanolamine species, although the latter were less abundant relative to the former than with islet GPE (not shown), and the contribution of arachidonate-containing plasmenylethanolamine species to the ESI/MS negative ion current profile for heart GPE species was about a third of that for islets (Table 1).

Glycerophosphocholine (GPC) lipids contain a quaternary nitrogen moiety with a fixed positive charge and are readily visualized in positive ion ESI/MS. Although negative ions can be formed from GPC species (*27*), the signal obtained from GPC species in negative ion mode under the conditions of ESI/MS analysis used in this study was much lower than that for GPE species in negative ion mode or for GPC species in positive ion mode, as summarized in Experimental Procedures. Positive ion ESI/MS analyses were therefore performed with lithiated adducts of islet GPC that had been isolated by NP-HPLC (Figure 7).

The two most abundant ions in the islet GPC−Li^+ total positive ion current profile occurred at *m*/*z* 788 and 816 (Figure 7A). The tandem mass spectra of the former (Figure 7B) indicated that it represented the $(MLi)^+$ ion of (16:0/20:4)-GPC (Figure 2E). Product ions that identify the headgroup include those generated by loss of trimethylamine (*m*/*z* 757) or by net loss of the phosphocholine headgroup with a proton (*m*/*z* 633) or a lithium ion (*m*/*z* 627). Ions

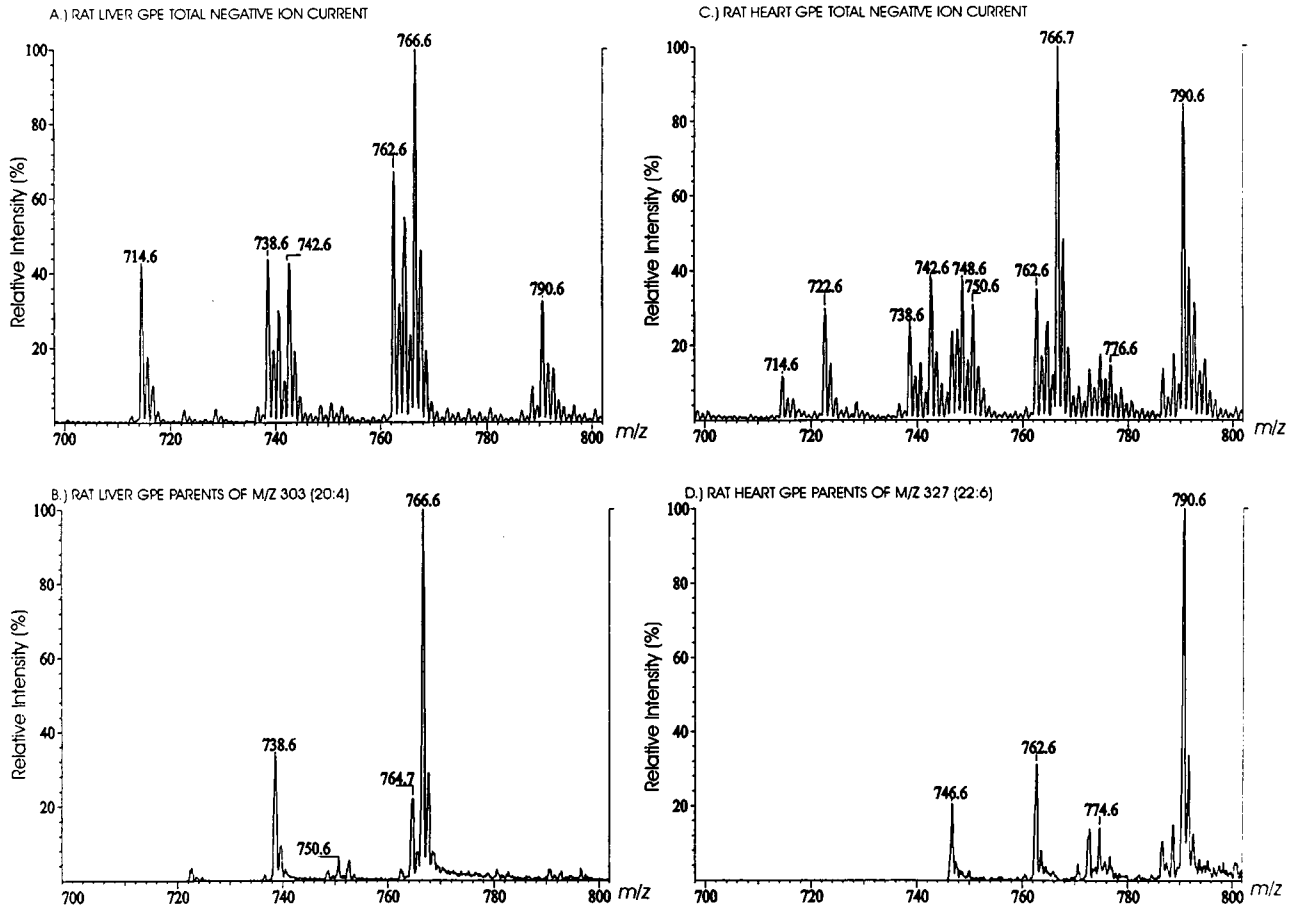

FIGURE 6: Electrospray ionization negative ion mass spectrometric analysis of glycerophosphoethanolamine lipids from rat liver and heart. Phospholipid extracts from rat liver (panels A and B) or heart (panels C and D) were analyzed by NP-HPLC to isolate GPE lipids, which were then analyzed by negative ion ESI/MS. Panels A (liver) and C (heart) are the total negative ion current profiles. Panels B (liver) and D (heart) represent a linked-scanning tandem MS experiments in which parent ions were identified that yield the arachidonate anion (*m*/*z* 303) (panel B) or the docosahexaenoate anion (*m*/*z* 327) (panel D) upon CAD.

that identify the fatty acid substituents include those at *m*/*z* 473 and 425, reflecting loss of trimethylamine and either the *sn*-1 or the *sn*-2 substituent, respectively. The former ion is characteristically more abundant than the latter, which permits assignment of fatty acid substituent positions (*43*). Another prominent ion (*m*/*z* 341) reflects loss of arachidonate as a ketene and net loss of phosphocholine with lithium ion (Figure 7B).

Similar features of the tandem spectrum of the ion at *m*/*z* 816 (Figure 7C) from the islet GPC−Li^+ mixture permit assignment of the parent species as (18:0/20:4)-GPC (Figure 2F). Both this spectrum (Figure 7C) and that of (16:0/20:4)-GPC−Li^+ (Figure 7B) contain an ion at *m*/*z* 473 that is common to the tandem spectra of arachidonate-containing GPC−Li^+ species (*43*) and generated by loss of trimethylamine plus the *sn*-1 substituent. Tandem MS scanning for parents of this ion identifies arachidonate-containing species in GPC−Li^+ mixtures (*43*), as illustrated in Figure 7D for islet GPC−Li^+ species. The three most prominent ions in this spectrum represent (16:0/20:4)-GPC−Li^+ (*m*/*z* 788), (18:1/20:4)-GPC−Li^+ (*m*/*z* 814), and (18:0/20:4)-GPC−Li^+. Comparison of Figure 7 panels A and D indicates that the most prominent components of islet GPC contain arachidonate.

Other GPC−Li^+ species identified from their tandem mass spectra in the islet mixture included (16:0/16:0)-GPC−Li^+ (*m*/*z* 740), (16:0/18:2)-GPC−Li^+ (*m*/*z* 764), (16:0/18:1)-GPC−Li^+ (*m*/*z* 766), and (18:0/18:2)-GPC−Li^+ (*m*/*z* 792). No prominent islet GPC−Li^+ species were observed with *m*/*z* values of 772, 770, or 744 (Figure 7A). Had such species been present, their $(M - 15)^-$ ions would be potential contributors to the ESI/MS negative ion current profile at *m*/*z* 750, 748, and 722, respectively. As summarized in Experimental Procedures, experiments with standards indicated a low yield of $(M - 15)^-$ ions from GPC species under our conditions of negative ESI/MS analysis compared to the yield of $(M - H)^-$ ions from equimolar amounts of GPE species. These observations, coupled with the very similar profile of GPE species obtained from crude islet extracts (Figure 1) and from NP-HPLC-purified islet GPE (Figure 4A), suggested that negative ion ESI/MS profiles of crude islet phospholipid extracts provide an adequate representation of islet GPE species. This approach was therefore used to characterize GPE species in islet subcellular membranes, which are obtainable in insufficient amounts to permit HPLC analyses without losses of labile analytes from the trace quantities of available phospholipids.

A subcellular membrane of critical importance to islet function is that bounding the insulin secretory granule, which fuses with the β-cell plasma membrane during insulin exocytosis. Arachidonate-containing plasmenylethanolamine molecules facilitate fusion of membrane bilayers by promoting formation of an intermediate inverted micellar structure (*23*). A rabbit brain cytosolic protein has been isolated and

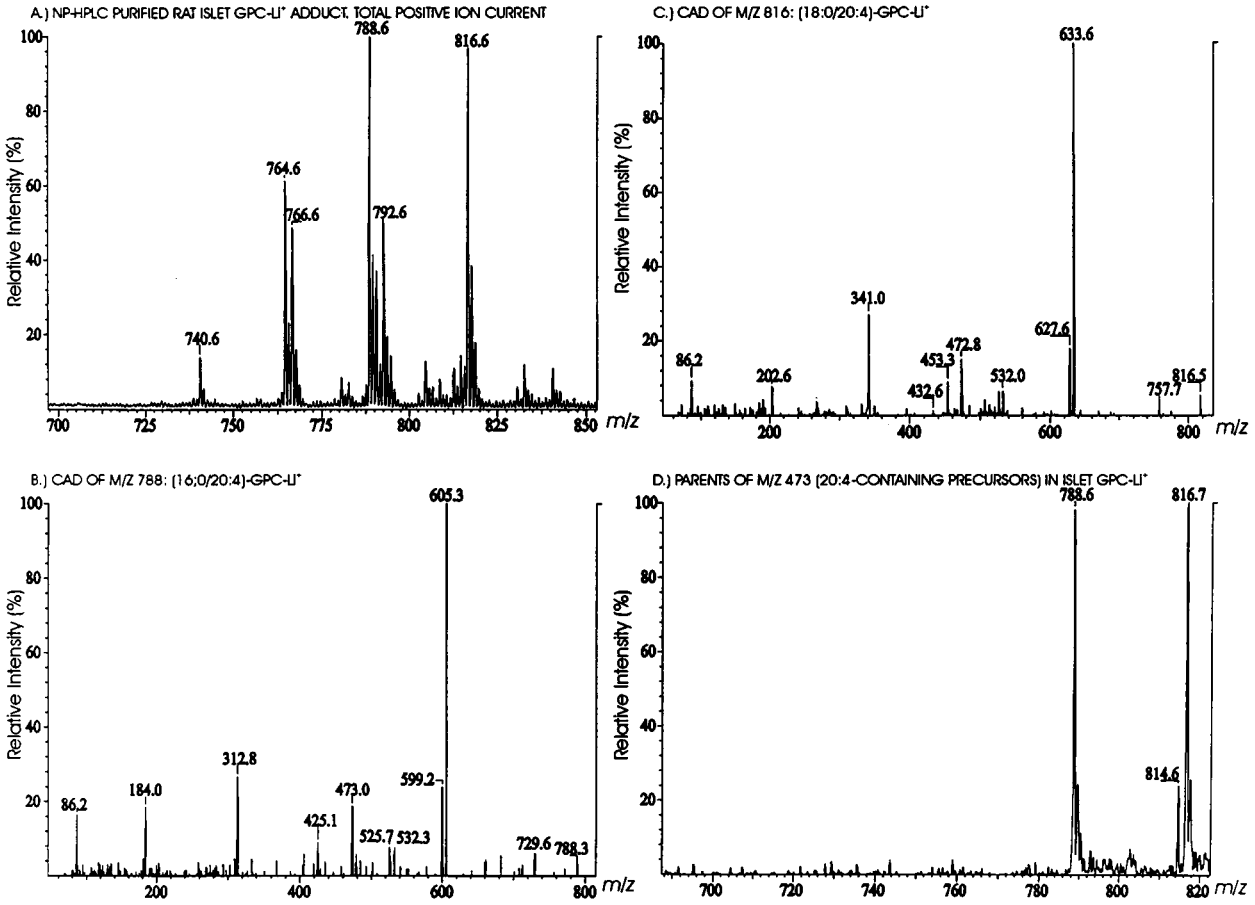

FIGURE 7: Electrospray ionization positive ion mass spectrometric analysis of glycerophosphocholine lipids from isolated rat pancreatic islets. Phospholipids extracted from isolated rat pancreatic islets were analyzed by NP-HPLC to isolate GPC lipids, which were then analyzed by positive ion ESI/MS as lithiated adducts. Panel A is the total positive ion current profile. Panels B and C are the tandem mass spectra obtained upon CAD of the parent ions at *m*/*z* 788 and 816, respectively. Panel D represents a tandem MS scanning experiment in which parent ions were identified that yield an ion at *m*/*z* 473 upon CAD.

characterized that specifically catalyzes fusion of model plasmenylethanolamine-containing membranes but is inactive against model membranes that do not contain plasmenylethanolamine (*24*). This factor and a similar factor from HIT insulinoma cells also catalyze fusion of islet plasma membranes and secretory granules (*44*).

The facts that the rabbit brain cytosolic factor requires plasmenylethanolamine in both membrane compartments undergoing fusion (*23*, *24*) and that it catalyzes fusion of islet secretory granule and plasma membranes (*44*) suggest that these membranes contain plasmenylethanolamine species. Previous studies involving two HPLC steps, solvolysis, derivatization, and GC/MS suggested that islet secretory granules contain little plasmenylethanolamine (*20*), but the content of such molecules may have underestimated because of losses during multiple processing steps of the trace amounts of secretory granule phospholipids obtainable. These phospholipids were therefore analyzed directly by ESI/MS after extraction from a secretory granule preparation that exhibited the expected (*34*, *20*) enrichment in insulin content, relative to homogenate, and no enrichment in 5′-nucleotidase activity (Table 2).

Table 2: Biochemical Characterization of Purified Insulin Secretory Granules[a]

fraction	composition	insulin content (milliunits/ μg of protein)	5′-nucleotidase activity (nmol/[h·μg of protein)])
H	homogenate	0.82	2.67
S_1	900*g* supernatant	2.05	1.20
P_1	900*g* pellet	0.59	3.20
S_2	13000*g* supernatant	0.61	0.56
P_2	13000*g* pellet	2.51	4.18
SG	secretory granules	18.55	1.23
M	non-SG membranes	0.93	6.84

[a] Pancreatic islets isolated from 6 rats were homogenized and the homogenate (H) was centrifuged (900*g*, 5 min) to yield a supernatant (S_1) and pellet (P_1). S_1 was centrifuged (13000*g*, 10 min) to yield a supernatant (S_2) and pellet (P_2). S_2 was applied to a Percoll density gradient and centrifuged (13000*g*, 10 min) to yield a population of secretory granules (SG) and non-SG membranes (M). Protein, insulin, and 5′-nucleotidase activity were measured in aliquots of each fraction. The tabulated experiment is representative of five. The observed enrichment in insulin in the SG fraction relative to H corresponds closely to previously reported values (*19*, *34*). The lack of enrichment in the SG fraction relative to H in 5′-nucleotidase activity contrasts to the 5-fold (*28*) to 13-fold (*19*) enrichment in this parameter obtained in purified islet plasma membrane preparations.

The negative ion ESI/MS profile of secretory granule phospholipids (Figure 8A) is similar to that from whole islets in Figure 4A and includes the arachidonate-containing plasmenylethanolamine species represented by ions at *m*/*z* 722 [(16:0p/20:4)-GPE], *m*/*z* 748 [(18:1p/20:4)-GPE], and *m*/*z* 750 [(18:0p/20:4)-GPE]. The similar relative intensities of these ions in Figures 4A and 8A indicates that arachidonate-containing plasmenylethanolamine species are similarly prominent components of secretory granule GPE and whole islet mixed membrane GPE. The positive ion ESI/MS profile

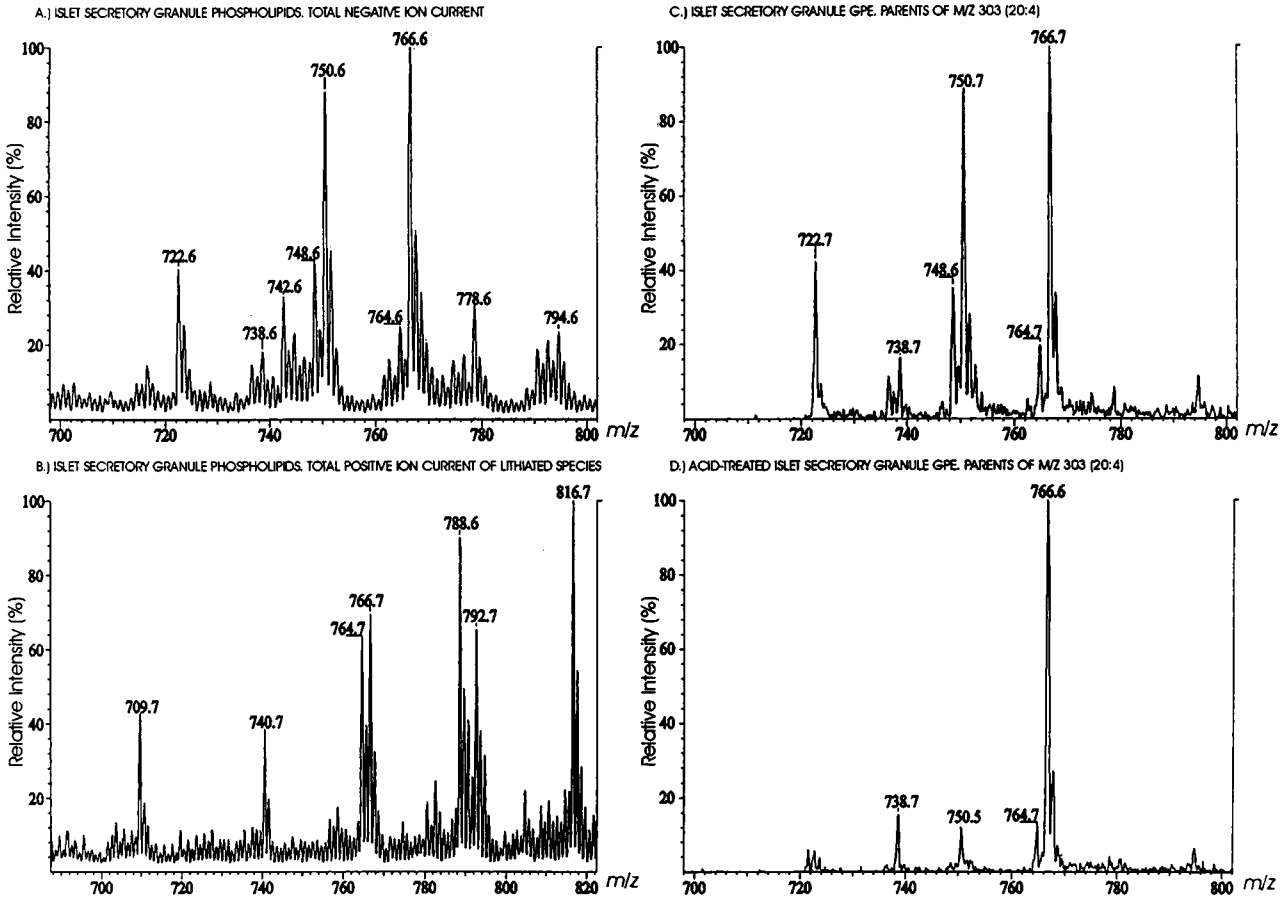

FIGURE 8: Electrospray ionization mass spectrometric analysis of phospholipids from isolated insulin secretory granules from pancreatic islets. Phospholipids were extracted from purified insulin secretory granules prepared from isolated rat islets and analyzed by ESI/MS. Panel A is the total negative ion current profile and panel B is the total positive ion current profile of lithiated adducts. Panels C and D represent negative ion tandem MS scanning experiments in which parent ions were identified from non-acid-treated (panel C) or acid-treated (panel D) secretory granule phospholipids that yielded arachidonate anion (*m*/*z* 303) as a product upon CAD.

of lithiated adducts of GPC species from secretory granule membranes (Figure 8B) is also similar to that from whole islet NP-HPLC-purified GPC (Figure 7A), except that an ion representing 16:0-sphingomyelin (*m*/*z* 709) is observed in the secretory granule phospholipids because GPC had not been isolated by NP-HPLC before ESI/MS analysis.

To confirm identification of arachidonate-containing plasmenylethanolamine species in secretory granules, tandem MS scanning experiments were performed to identify parents that yield an arachidonate anion (*m*/*z* 303) upon CAD. Such scans (Figure 8C) yielded a profile similar to that for the ESI/MS total negative ion current profile of secretory granule phospholipids (Figure 8A), indicating that the most prominent components of secretory granule GPE contain arachidonate. In Figure 8C, the ions at *m*/*z* 722, 748, and 750 represent plasmenylethanolamine species and those at *m*/*z* 738, 764, and 766 represent diacyl-GPE species. Exposure of secretory granule phospholipids to acid resulted in about a 10-fold decrement in intensities of ions representing plasmenylethanolamine species relative to the ions representing diacyl-GPE species (Figure 8D), confirming the assignments of the plasmalogen species.

Negative ion ESI/MS analyses of phospholipids in plasma membranes from rat islets revealed a similar prominence of arachidonate-containing plasmenylethanolamine species (Table 3). Contrary to previous estimates (*20*), therefore, direct ESI/MS analyses indicate that arachidonate-containing plasmenylethanolamine species are prominent components of both islet secretory granule and plasma membrane GPE, and this may account for the ability of the plasmenylethanolamine-requiring factor from rabbit brain (*24*) to catalyze fusion of these membranes (*44*).

Activity of a similar fusion factor in HIT-T15 insulinoma cell cytosol is illustrated in Figure 9. Isolated insulin secretory granules were labeled with the fluorophore octadecylrhodamine (R18) and mixed with unlabeled islet plasma membranes. In this system, fusion of unlabeled and R18-labeled membranes results in fluorophore dilution, relief of self-quenching, and increased fluorescence (*41*). As illustrated in Figure 9 (tracing CON), little fusion occurs upon simple mixing of R18-labeled secretory granules and unlabeled plasma membranes. To this assay system were then added aliquots of eluant from DE-52 anion-exchange chromatographic analysis of HIT-T15 insulinoma cell cytosol. Aliquots of a specific fraction of eluant induced a fusion response (tracing FB), whereas aliquots of earlier- (tracing FA) or later-eluting (tracing FC) fractions did not. Because the islet membranes in these experiments were prepared from rats, we examined whether rat tissues express a similar fusion-catalyzing factor by preparing rat brain cytosol and analyzing it by DE-52 anion-exchange chromatography. As illustrated in the inset in Figure 9, fusion-catalyzing activity was expressed in rat brain cytosol and eluted with a chromatographic profile similar to that reported (*24*) for the

Table 3: Summary of Glycerophosphoethanolamine Molecular Species Identified in Rat Pancreatic Islet Subcellular Membranes by Electrospray Ionization Negative Ion Tandem Mass Spectrometry[a]

		relative intensity			
m/*z*	assignment	rat whole islet mixed membranes	rat islet secretory granules	rat islet plasma membranes	rat islet endoplasmic reticulum
700	16:0p/18:1-GPE	00	01	00	01
714	16:0/18:2-GPE	00	01	00	01
716	16:0/18:1-GPE	00	06	03	01
722	16:0p/20:4-GPE	36	37	48	54
728	18:0p/18:1-GPE	00	02	00	00
738	16:0/20:4-GPE	12	12	07	03
742	18:0/18:2-GPE	17	26	16	15
746	16:0p/22:6-GPE	00	02	11	04
748	18:1p/20:4-GPE	28	38	32	33
750	18:0p/20:4-GPE	59	87	100	100
762	16:0/22:6-GPE	14	02	00	00
764	18:1/20:4-GPE	21	20	16	13
766	18:0/20:4-GPE	100	100	98	64
774	18:0p/22:6-GPE	07	08	09	08
776	18:0p/22:5-GPE	06	10	06	05
778	18:0p/22:4-GPE	24	17	14	05
790	18:0/22:6-GPE	11	10	07	05
792	18:0/22:5-GPE	04	11	05	00
794	18:0/22:4-GPE	17	13	10	03
	Fraction of Tabulated GPE ion Current Represented by				
	20:4-containing species	0.72	0.73	0.79	0.85
	plasmalogen species	0.45	0.50	0.58	0.66
	plasmalogens with 20:4	0.35	0.40	0.47	0.59

[a] Bligh-Dyer lipid extracts from whole islet mixed membranes and from each rat islet subcellular membrane preparation were analyzed by negative ion ESI/MS as in Figure 1. The relative intensities of $(M - H)^-$ ions corresponding to GPE species were determined from the total negative ion current profile. The identities of the molecular species represented by the $(M - H)^-$ ions were determined by CAD of individual parent ions and tandem MS. Assignments were confirmed by linked-scanning tandem MS experiments to identify parents of specific fatty acid carboxylate anions. The notation identifying the molecular species is as in Table 1. Minor isobaric contributors to some of the ions in the total ion current have not been included in the table.

rabbit brain fusion factor.

DISCUSSION

These studies indicate that arachidonate-containing molecular species are the most prominent components of the major phospholipid headgroup classes in islets, including GPI, GPS, GPE, and GPC. This is consistent with previous GC/MS analyses suggesting that arachidonate is the predominant *sn*-2 substituent in islet phospholipids (*19*, *20*), and the apparent relative abundances of the major islet GPE and GPC species identified here, as estimated from their contribution to ESI/MS total ion current profiles, is similar to that estimated from the fatty acid content of these species after HPLC isolation, solvolysis, derivatization, and GC/MS analyses (*19*, *20*). The ESI/MS analyses here were performed with intact phospholipid molecules, however, and thus permit direct structural assignments that avoid indirect inferences of identities of phospholipid species inherent in HPLC and GC/MS-based methods. For each islet phospholipid species identified by ESI/MS, the tandem mass spectrum contained ions that identified both the fatty acid substituents and the headgroup.

Arachidonate-containing species contribute a greater fraction of the ESI/MS negative ion current profile for GPE in islets than in liver, heart, or brain, and about half of the ion current from arachidonate-containing GPE species in islets is attributable to plasmenylethanolamine species. The fraction of the GPE ion current contributed by plasmenylethanolamine species in islets exceeds that for liver or heart and is similar to that for brain. In brain, docosahexaenoate-containing plasmenylethanolamine species contribute a greater fraction of the GPE negative ion current profile than do arachidonate-containing plasmenylethanolamine species, in contrast to the case for islet GPE. The prominence of arachidonate-containing plasmenylethanolamine species in islets is therefore not a general feature of GPE in the rat tissues examined.

The identification of the islet plasmenylethanolamine species here rests in part on their tandem mass spectra, which contain ions that identify the headgroup and the fatty acid substituent. Although the ether-linked *sn*-1 substituent does not yield an ion that directly identifies it in the spectrum, the existence of such a substituent can be inferred from the *m*/*z* value of the $(M - H)^-$ ion and the presence of only a single fatty acid carboxylate anion in the spectrum. These features do not, however, distinguish alkyl-ether GPE species from plasmenylethanolamine species (*27*). For example, the plasmalogen species 18:0p/20:4-GPE is isomeric with the alkyl-ether GPE species with residues of oleic alcohol and arachidonic acid as the *sn*-1 and *sn*-2 substituents, respectively. Both species would yield identical *m*/*z* values for $(M - H)^-$ ions and for product ions reflecting the *sn*-2 substituent and the headgroup.

The alkyl-ether and the plasmalogen species are, however, distinguished by sensitivity to acid, since the former is acid-stable and the latter is acid-labile (*24*, *39*). Each species identified as a plasmenylethanolamine in islets and other tissues here exhibited acid lability. The islet plasmenylethanolamine species so identified are consistent with those previously identified in studies that involved HPLC isolation of individual phospholipid molecular species, acid methanolysis, and GC/MS analyses (*19*, *20*). Acid methanolysis yields dimethylacetals from the *sn*-1 fatty aldehyde substituents of plasmalogens (*19*, *20*, *45*, *46*) but not from alkyl-ether *sn*-1 substituents (*45*, *46*). This and previous studies (*19*, *20*) therefore yield unequivocal identification of the major plasmenylethanolamine species in islets.

The ESI/MS analyses described here have the advantage over previous approaches to identification of plasmenylethanolamine species that fewer processing steps are involved, and losses of these labile compounds are therefore minimized. This is particularly important with trace quantities of phospholipid mixtures, such as those from isolated insulin secretory granules, and this probably accounts for the finding here that arachidonate-containing plasmenylethanolamine species are prominent components of secretory granule membrane GPE, while previous, indirect analyses suggested that secretory granule GPE consisted predominantly of diacyl species and contained little plasmenylethanolamine (*20*).

The contribution of arachidonate-containing plasmenylethanolamine species to ESI/MS negative ion current profiles for secretory granule GPE is in fact at least as high as that for whole rat islet mixed membrane GPE, and this is also true for islet plasma membrane GPE and for human islet mixed membrane GPE. The similar prominence of arachidonate-containing plasmenylethanolamine species in GPE of islets from two species, the fact that this is not a general feature of rat tissue GPE, and the fact that such molecules

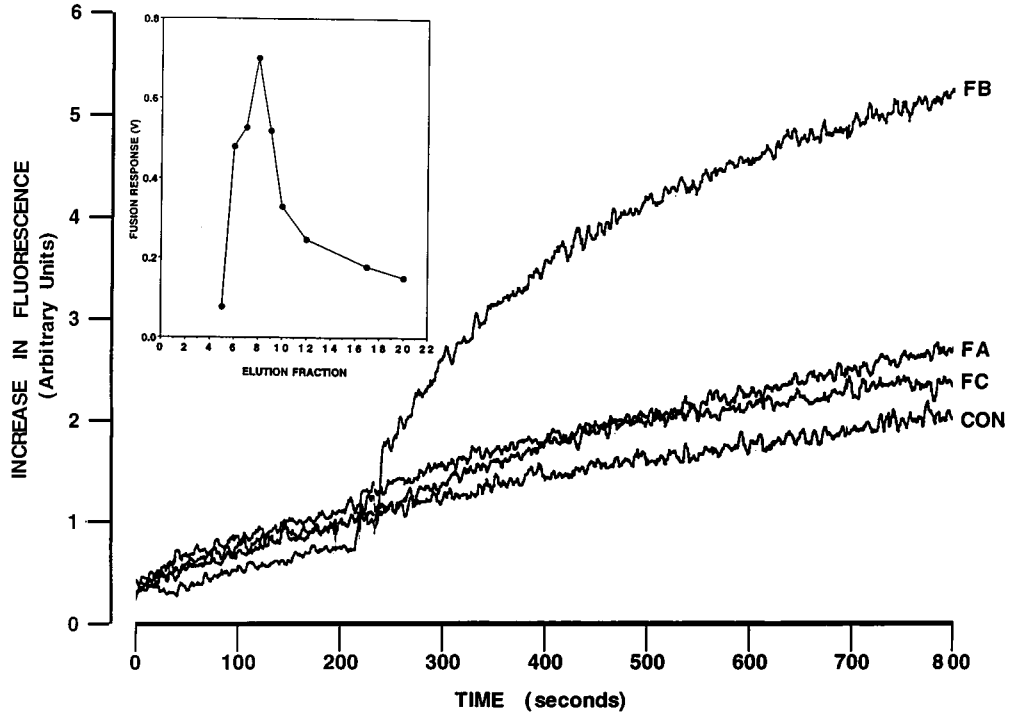

FIGURE 9: Catalysis of fusion of isolated insulin secretory granules and isolated islet plasma membranes by components of cytosol from HIT-T15 insulinoma cells and from rat brain after resolution from other cytosolic components by anion-exchange chromatography. Purified insulin secretory granules were labeled with octadecylrhodamine (R18) and mixed with unlabeled, purified islet plasma membranes in the chamber of a spectrofluorometer. Fusion of these membranes results in relief of self-quenching and an increase in fluorescence. The tracing labeled CON illustrates that little spontaneous fusion occurs. Cytosol prepared from HIT-T15 insulinoma cells was analyzed by anion-exchange chromatography on a DE-52 column, and aliquots of eluant fractions A−C were added to the fusion system. The tracing labeled FB illustrates that fusion of the membranes is catalyzed by an aliquot of fraction B. The tracings labeled FA and FC illustrate that no such effect occurs with aliquots of earlier- or later-eluting fractions, respectively. In the inset, cytosol prepared from rat brain was similarly analyzed by anion-exchange chromatography, and aliquots of eluant fractions were added to the fusion system. The fusion response on the ordinate reflects the difference between fluorescence signal obtained 600 s after addition of an aliquot of eluant fractions and signal obtained 600 s after addition of buffer only.

are prominent components of islet subcellular membranes that participate in insulin secretion raise the possibility that these molecules may participate in β-cell secretory function.

Insulin secretion requires fusion of secretory granule and plasma membranes. Fusion of model membranes is favored by the presence of plasmenylethanolamine constituents, particularly arachidonate-containing species (*23*). This may reflect the propensity of such molecules to adopt an inverted micellar phase (*25*) intermediate structure in the fusion of membrane bilayers (*26*). A factor isolated from rabbit brain cytosol specifically catalyzes fusion of plasmenylethanolamine-containing model membranes and fails to catalyze fusion of similar membranes that do not contain such molecules (*24*). This factor exhibits chromatographic, immunochemical, and amino acid sequence similarities to glyceraldehyde-3-phosphate dehydrogenase (GAPDH), and its fusion-catalyzing activity is prevented by an anti-GAPDH antibody (*24*). This factor also catalyzes fusion of islet secretory granule and plasma membranes, and this is prevented by anti-GAPDH antibody or by treating the islet membranes with acid to destroy plasmenylethanolamine species (*44*).

These findings initially seemed discrepant with the requirement of the fusion factor for plasmenylethanolamine-containing membranes (*24*) because HPLC and GC/MS measurements had indicated that insulin secretory granule membranes contained little plasmenylethanolamine (*20*). The ESI/MS findings here that arachidonate-containing plasmenylethanolamine species are actually prominent components of insulin secretory granule and plasma membrane GPE may explain this apparent discrepancy. Whether the rabbit brain factor catalyzes membrane fusion in vivo remains to be established, but HIT-T15 insulinoma cell cytosol contains a similar factor with fusion-catalyzing activity (*44*). Our findings indicate that the chromatographic behavior of this HIT-T15 cell factor and of a fusion factor from rat brain is similar to that of the rabbit brain factor (*24*), but it is not yet known whether β-cell and rat brain fusion-catalyzing activities reside in GAPDH isoforms.

Although arachidonate-containing plasmenylethanolamine species may play structural roles in β-cell membrane function, such species are also expressed in some nonsecretory cells (*29*) and may play additional roles in cell biology. In addition, arachidonate-containing species are prominent components of islet phospholipid headgroup classes other than GPE. Of the total islet arachidonate content, about 31% resides in GPE, 53% in GPC, 10% in GPI, and 3% in GPS (*19*, *20*). Another function of islet arachidonate-containing phospholipids may be to serve as substrates for phospholipases activated when islets are stimulated with glucose. Glucose induces hydrolysis of arachidonate from islet phospholipids and accumulation of nonesterified arachidonate and smaller amounts of other free fatty acids (*9*, *10*).

Islets express at least three distinct PLA_2 enzymes that may participate in glucose-induced hydrolysis of arachidonate from phospholipids, including an 84 kDa, cytosolic, Ca^{2+}-

independent PLA_2 (iPLA_2) (*47*), an 85 kDa cytosolic Ca^{2+}-dependent PLA_2 (cPLA_2) (*17*, *48*−*51*), and low molecular weight Ca^{2+}-dependent secretory PLA_2 (sPLA_2) (*52*) associated with insulin secretory granules (*53*). It has been suggested that arachidonate liberated by sequential activation of these enzymes may play distinct roles in various steps of the exocytotic process (*54*). Much interest has focused on the potential role of arachidonate in modulating β-cell cytosolic [Ca^{2+}]. Arachidonate induces release of Ca^{2+} from β-cell intracellular sequestration sites (*9*), facilitates extracellular Ca^{2+} entry into β-cells (*13*, *14*, *16*, *55*), and amplifies the rise in both β-cell cytosolic [Ca^{2+}] (13) and insulin secretion (*10*) induced by depolarization. Such effects may be mediated by arachidonate-sensitive ion channels (*56*−*59*) and contribute to early β-cell signaling responses to glucose (*12*).

A potential role for arachidonic acid in distal exocytotic events has also been suggested (*60*−*63*). Fusion of secretory granule and plasma membranes can be induced by treating plasma membranes with sPLA_2 isozymes (*60*, *62*, *63*), such as those in secretory granules of several cells (*64*−*66*) including islet β-cells (*53*), although no spontaneous fusion occurs in such systems. Treating these membranes with sPLA_2 induces arachidonate release, and depleting the nonesterified arachidonate content of the sPLA_2-treated membranes with serum albumin suppresses the fusion response, while exogenous arachidonate amplifies it (*62*, *63*). One function of sPLA_2 in secretory granules may thus be to modify plasma and/or secretory granule membranes by increasing their nonesterified arachidonate content so as to promote fusion.

Although the precise roles of arachidonic acid and the phospholipids that contain it in β-cell biology are not yet clearly established, the findings reported here provide additional evidence that arachidonate-containing phospholipids are prominent components of islet cell membranes. These compounds may play structural roles in the functions of such membranes and may serve as substrates for β-cell phospholipases activated in signal transduction processes underlying insulin secretion.

ACKNOWLEDGMENT

We thank Dr. Bruce Patterson for access to his spectrofluorometer and Dr. Mary Mueller, Sheng Zhang, and Z. Hu for excellent technical assistance.

REFERENCES

1. Porte, D. (1991) *Diabetes 40*, 166−180.
2. Meglasson, M. D., and Matschinsky, F. M. (1986) *Diabetes/Metab. Rev. 2*, 163-214.
3. Matschinsky, F. M. (1990) *Diabetes 39*, 647−652.
4. Cook, D. L, and Hales, C. N. (1984) *Nature 311*, 271−273.
5. Arkhammar, P., Nilsson, T., Rorsman, P., and Berggren, P. O. (1987) *J. Biol. Chem. 262*, 5448−5454.
6. Gylfe, E. (1988) *J. Biol. Chem. 263*, 5044−5048.
7. Misler, S., Barnett, D. W., Gillis, K. D., and Pressel, D. M. (1992) *Diabetes 41*, 1221−1228.
8. Misler, S., Barnett, D. W., Gillis, K. D., Scharp, D. W., and Falke, L. C. (1992) *Diabetes 41*, 662−670.
9. Wolf, B. A., Turk, J., Sherman, W. R., and McDaniel, M. L. (1986) *J. Biol. Chem. 261*, 3501−3511.
10. Wolf, B. A., Pasquale, S. M., and Turk, J. (1991) *Biochemistry 30*, 6371−6379.
11. Metz, S. A. (1991) *Diabetes 40*, 1565−1573.
12. Turk, J., Gross, R. W., and Ramanadham, S. (1993) *Diabetes 42*, 367−374.
13. Ramanadham, S., Gross, R. W., and Turk, J. (1992) *Biochem. Biophys. Res. Commun. 184*, 647−653.
14. Metz, S. A., Draznin, B., Sussman, K. E., and Leitner, J. W. (1987) *Biochem. Biophys. Res. Commun. 142*, 251−258.
15. Konrad, R. J., Jolly, Y. C., Major, C., and Wolf, B. A. (1992) *Biochim. Biophys. Acta 1135*, 215−220.
16. Ramanadham, S., Gross, R. W., Han, X., and Turk, J. (1993) *Biochemistry 32*, 337−346.
17. Loweth, A. C., Scarpello, J. H. B., and Morgan, N. G. (1996) *Biochem. Biophys. Res. Commun. 218*, 423−427.
18. Thams, P., and Capito, J. (1997) *Biochem. Pharmacol. 53*, 1077−1086.
19. Ramanadham, S., Bohrer, A., Mueller, M., Jett, P., Gross, R. W., and Turk, J. (1993) *Biochemistry 32*, 5339−5351.
20. Ramanadham, S., Bohrer, A., Gross, R. W., and Turk, J. (1993) *Biochemistry* 32, 13499−13509.
21. Freysz, L. F., Beith, R., Judes, C., Sensenbrenner, M., Jacob, M., and Mandel, P. J. (1968) *J. Neurochem. 15*, 307−313.
22. Atouf, F., Czernichow, P., and Scharfman, R. (1997) *J. Biol. Chem. 272*, 1929−1934.
23. Glaser, P. E., and Gross, R. W. (1994) *Biochemistry 33*, 5805−5812.
24. Glaser, P. E., and Gross, R. W. (1995) *Biochemistry 34*, 12193−12203.
25. Han, X., and Gross, R. W. (1992) *Biophys. J. 63*, 309−316.
26. Cullis, P. R., and Hope, M. J. (1991) in *Biochemistry of Lipids, Lipoproteins, and Membranes*, Elsevier, Amsterdam.
27. Murphy, R. C., and Harrison, K. A. (1994) *Mass Spectrom. Rev. 13*, 57−76.
28. McDaniel, M. L., Colca, J. R., Kotagal, N., and Lacy, P. E. (1983) *Methods Enzymol. 98*, 182−200.
29. Han, X., and Gross, R. W. (1994) *Proc. Natl. Acad. Sci. U.S.A. 91*, 10635−10639.
30. Han, X., and Gross, R. W. (1995) *J. Am. Soc. Mass Spectrom. 6*, 1202−1210.
31. Han, X., and Gross, R. W. (1996) *J. Am. Chem. Soc. 118*, 451−457.
32. Han, X., Gubitosi-Klug, R. A., Collins, B. J., and Gross, R. W. (1996) *Biochemistry 35*, 5822−5832.
33. Ricordi, C., Lacy, P. E., Finke, E. H., Olack, B. J., and Scharp, D. W. (1988) *Diabetes 37*, 413−420.
34. Jones, P. M., Saermark, T., and Howell, S. I. (1987) *Anal. Biochem. 166*, 142−149.
35. Naber, S. P., McDonald, J. M, Jarrett, L., Ludvigsen, C. W., and Lacy, P. E. (1980) *Diabetologia 19*, 439−446.
36. Avruch, J., and Wallach, D. F. H. (1971) *Biochim. Biophys. Acta 233*, 334−347.
37. Bligh, E. G., and Dyer, W. J. (1959) *Can. J. Biochem. Physiol. 37*, 911−917.
38. Patton, G. M., Fasulo, J. M., and Robins, S. J. (1982) *J. Lipid Res. 23*, 190−196.
39. Kayganich, K. A., and Murphy, R. C. (1994) *Anal. Chem. 64*, 2965−2971.
40. Ramanadham, S., Wolf, M., Jett, P. A,. Gross, R. W., and Turk, J. (1994) *Biochemistry 33*, 7442−7452.
41. Hoekstra, D., de Boer, T., Klappe, K., and Wilshut, J. (1984) *Biochemistry 23*, 5675−5681.
42. Horrocks, L. A., and Sharma, M. (1982) in *Phospholipids* (Hawthorne, G., and Ansell, G. B., Eds.) pp 51−93, Elsevier Biomedical Press, Amsterdam.
43. Hsu, F. F., Bohrer, A., and Turk, J. (1998) *J. Am. Soc. Mass Spectrom.* (in press).
44. Han, X., Ramanadham, S., Turk, J., and Gross, R. W. (1998) *Biochem. J.* (submitted for publication).
45. Gross, R. W. (1984) *Biochemistry 23*, 158−165.
46. Gross, R. W. (1985) *Biochemistry 24*, 1662−1668.
47. Ma, Z., Ramanadham, S., Kempe, K., Chi, X. S., Ladenson, J., and Turk, J. (1997) *J. Biol. Chem. 272*, 11118−11127.
48. Dunlop, M., and Clark, S. (1995) *Int. J. Biochem. Cell Biol. 27*, 1191−1199.
49. Loweth, A. C., Scarpello, J. H. B., and Morgan, N. G. (1995) *Mol. Cell. Endocrinol. 112*, 177−183.

50. Chen, M., Yang, Z. D., Naji, A., and Wolf, B. A. (1996) *Endocrinology 137*, 2901−2909.
51. Parker, K. J., Jones, P. M., Hunton, C. H., Persaud, S. J., Taylor, S. G., and Howell, S. I. (1996) *J. Mol. Endocrinol. 17*, 31−43.
52. Metz, S. A., Holmes, D., Robertson, R. P., Leitner, W., and Draznin, B. (1991) *FEBS Lett. 295*, 110−112.
53. Ramanadham, S., Ma, Z., Arita, H., Zhang, S., and Turk, J. (1998) *Biochim. Biophys. Acta* (in press).
54. Jolly, Y. C., Major, C., and Wolf, B. A. (1993) *Biochemistry 32*, 12209−12217.
55. Ramanadham, S., and Turk, J. (1994) *Cell Calcium 15*, 259−264.
56. Vacher, P., McKenzie, J., and Dufy, B. (1989) *Am. J. Physiol. 257*, E203−211.
57. Miller, B., Sarantis, M., Traynelis, S. F., and Atwell, D. (1993) *Nature 355*, 722−725.
58. Petrou, S., Ordway, R. W., Singer, J. J., and Walsh, J. U. (1993) *Trends Biochem. Sci. 18*, 41−42.
59. Eddlestone, G. T. (1995) *Am. J. Physiol. 268*, C181−190.
60. Karli, W. O., Schafer, T., and Burger, M. M. (1990) *Proc. Natl. Acad. Sci. U.S.A. 87*, 5912- 5915.
61. Kudo, I., Murakami, M., Hara, S., and Inoue, K. (1993) *Biochim. Biophys. Acta 17*, 217−231.
62. Nagao, T., Kubo, T., Fujimoto, R., Nishio, H., Takeuchi, T., and Hata, F. (1995) *Biochem. J. 307*, 563−569.
63. Nishio, H., Takeuchi, T., Hata, F., and Yagasaki, O. (1996) *Biochem. J. 318*, 981−987.
64. Mounier, C., Faili, A., Vargaftig, B. B., Bon, C., and Hatmi, M. (1993) *Eur. J. Biochem. 216*, 169−175.
65. Chock, S. P., Schmauder-Chock, E. A., Cordella-Miele, E., Miele, L., and Mukherjee, A. B. (1994) *Biochem. J. 300*, 619−622.
66. Rosenthal, M. D., Gordon, M. N., Buescher, E. S., Slusser, J. H., Harris, L. K., and Franson, R. C. (1995) *Biochem. Biophys. Res. Commun. 208*, 650−656.

BI9722507